Development of Sodium Silicate Adhesives for Electrical Steel Bonding

by

Jordan Marks

Submitted to the
Department of Materials Science and Engineering
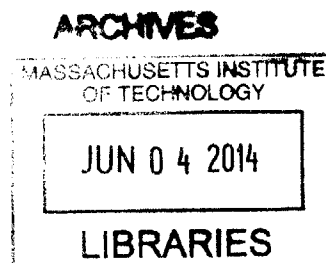in Partial Fulfillment of the Requirements for the Degree of

Bachelor of Science

at the

Massachusetts Institute of Technology

June 2014

© 2014 Marks
All Rights Reserved

The author hereby grants to MIT permission to reproduce and distribute publicly paper and electronic copies of this thesis document in whole or in part in any medium now known or hereafter created.

Signature redacted

Signature of Author ....

/ Jordan Marks
Department of Materials Science and Engineering
2 May 2014

Signature redacted

Certified by ....

Thomas Eagar
Professor of Materials Science and Engineering
Thesis Supervisor

Signature redacted

Accepted by ....

Professor Jeffrey C. Grossman
Undergraduate Committee Chairman

Development of Sodium Silicate Adhesives for Electrical Steel Bonding

by

Jordan Marks

Submitted to the
Department of Materials Science and Engineering
on 2 May 2014 in Partial Fulfillment of the
Requirements for the Degree of Bachelor of Science in
Materials Science and Engineering

ABSTRACT

Inorganic adhesives have several benefits over traditional joining methods for joining electrical steels used in magnetic cores of numerous industrial applications. As insulators with very high melting temperatures, the adhesives offer the possibility of increasing the efficiency of these machines. The aim of this project was to characterize sodium silicates as adhesives for such applications and develop methodology for their processing. The chemical and physical properties of the water-soluble sodium silicates were easily altered by changing the composition of Na_2O, SiO_4, and water, offering a spectrum of properties to investigate. Several aspects of the electrical steel provided by POSCO were also investigated, including surface chemistry and microstructure due to processing of the steel sheets. Coating efficacy was evaluated based on the adhesive's ability to wet the substrate to form a uniform coating, as well as resistance to mechanical loads, including adhesion and flexural strain. Greater degree of alkalinity in the sodium silicates resulted in improved wetting, uniformity, adhesion, and flexural strain for the range of viscosities that supported these behaviors. The microstructure of the electrical steels influenced the interaction of the adhesive with the surface, but properties still improved with higher alkalinity. Firing parameters were used to alter the mechanical properties of the silicates, as well as to determine operability limits. The best mechanical properties occurred for those coupons fired between 600°C and 800°C. The efficacy did not degrade significantly with long exposure to high temperatures, offering promise for sodium orthosilicates as appropriate adhesives for the described applications. Further study of the environmental conditions under which the adhesives will be used, as well as full characterization of the insulating properties will allow the processes developed here to be scaled up for industrial use.

Thesis Supervisor: Thomas Eagar
Title: Professor of Materials Science and Engineering

Table of Contents

Table of Figures

1. Introduction

1.1. Project Motivation and Background

Electrical steels are used in the magnetic cores of many machines including motors, generators, and transformers. Efforts to make these cores useful for energy efficient machines provide significant motivation to develop improved steels with lower core energy loss. One means of energy loss is eddy current loss through the steel sheets. This loss component may be reduced through the use of insulating coatings to ensure that the current is restricted to individual laminations. As a result, the magnetic cores usually consist of alternating layers of electrical steel with insulating material (Figure 1).
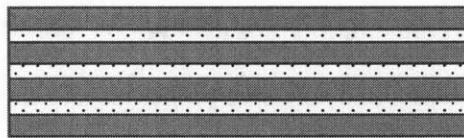
Figure 1. Layers of electrical steel (gray) separated by insulating layer (dots) to reduce energy loss.

Several methods of joining the sheets with insulating layers have been explored. One of these solutions involves applying an insulating coating film to the metal sheets. After coating, most core sheets are assembled by welding and interlocking processes. However these joining processes introduce stress concentrations that may degrade magnetic properties and have the potential to damage the metal core, compromising the electrical properties of the system. Additionally, thermal deformation resulting from welding may lead to degradation of magnetic characteristics and destruction of the insulating layers, making welding an unsuitable joining method.

Adhesive bonding offers numerous potential advantages as an alternative joining method, as adhesives can act to both insulate and join the sheets. No stress concentrations result from the joining process because the entire surface is bonded. As a low temperature process, no thermal

deformation due to heating occurs in the sheets. Adhesives also damp vibrations in these systems because they eliminate gaps between metal sheets, increasing fatigue resistance. Furthermore, adhesives are relatively lightweight and can be inexpensive. These benefits and others have encouraged companies to look into adhesives for electrical steel bonding, both pursuing various adhesive types and developing processes to apply the adhesive onto the surface to control homogeneity and maintain process efficiency.

Some companies, including Thyssen Krupp Steel EBG and Kawasaki Steel, have developed organic adhesive coatings for electrical steel, using thermoplastic synthetic resins and epoxy resins. A striking limitation of these organic coatings is restricted operating range, as most organic adhesives melt below a relatively low temperature for machine applications (200-300°C), undermining their insulating and adhesive properties and causing electrical shorts between the metal layers. Further, these adhesives may be susceptible to attack by some solvents. Inorganic adhesives offer the potential of improved environmental resistance due to high melting temperatures and their generally low reactivity. As higher temperatures can be realized, the efficiency of the machines will increase. For these applications, a suitable inorganic adhesive must be developed that will bond well to the surface of the electrical steel, producing a uniform coating which yields reliable mechanical and electrical properties.

2. Theoretical Background

2.1. Adhesion Fundamentals

Adhesive bonding is driven by two mechanisms involving the substrates and adhesive material: surface tension and mechanical interlocking. When an adhesive is applied between substrates, the pressure is lower in the adhesive than in the surrounding area (Figure 2). The pressure differential between the outside and inside of the adhesive pulls the substrates together. This effect is describe by Equation 1.

$$\rho_L - \rho_A = \gamma_{LV^0}\left(\frac{1}{R} - \frac{1}{r}\right) \qquad \text{(Equation 1)}$$

where ρ_L and ρ_A are the pressures in the liquid and the air respectively, γ_{LV^0} is the liquid surface tension, R is the radius of the area of contact with the solid, and r is the meniscus of the adhesive of thickness d such that $r = \frac{d}{2}$. It can be seen from this equation that if $r<<R$, $\rho_L - \rho_A$ will have a large negative magnitude, so there will be a much greater pressure surround the liquid than within it; thus the pressure increases with thinner joints.
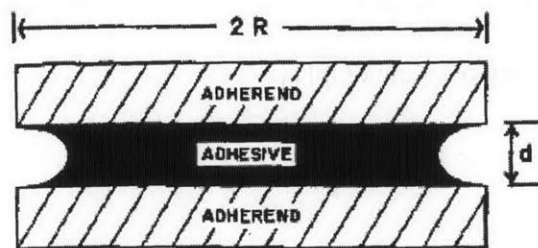
Figure 2. Surface Tension brings the substrates together when joined with an adhesive. Image courtesy of [1].

A very thin joint is not always practical due to surface roughness. In practice, it is nearly impossible to rid surfaces of all roughness, particularly when considering an atomic scale; this surface roughness interferes with the surface tension effect described above. Because only the surface asperities are in contact, the actual contact area is much smaller than the total area of the

bond (Figure 3), reducing the bond strength. Thicker joints mitigate this effect, as they "cover" the asperities, though this reduces the surface tension.
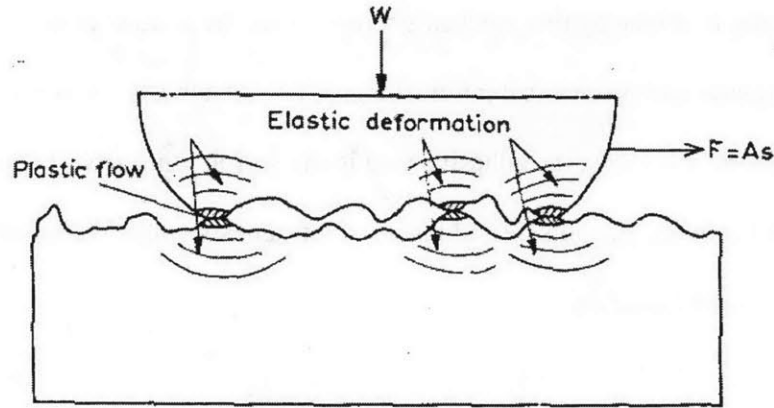
Figure 3. Actual Contact area between rough surfaces is significantly reduced. Image courtesy of [1].

Mechanical interlocking caused by surface roughness may be used advantageously in adhesive joint design. Rough surfaces have higher surface energy than smooth surfaces, making it easier to bond to the surface, as well as increasing contact area available for bonding. Bonds on rough surfaces inevitably contain pores or gas bubbles, as the adhesive can spread to certain voids easier than others. A greater extent of penetration increases adhesion because the bonded surface area is increased. This process is driven by capillary forces and can be approximated with the capillary rise equation [1]:

$$h \propto \frac{\gamma \cos \theta}{\rho r} \qquad\qquad \text{(Equation 2)}$$

where h is the height of penetration, γ is the liquid-air surface tension, θ is the contact angle, ρ is the density of the liquid, and r is the radius of the capillary. The extent of penetration depends on both the surface tension, which is governed by the adhesive, and the radius of the asperities, determined by the substrate. The capillary rise assumption simplifies the geometry of the interface plane; in practice the extent of penetration is more complicated. However, the

simplification does illuminate the crucial point that penetration is maximized with a high liquid-air surface tension and thus low contact angle. Adhesives with high contact angles do not flow easily over the surface to fill the crevices; these difficulties are amplified by viscous adhesives, which solidify shortly after application.

To continue the process of crevice penetration and to minimize the pores in a given bond, a low viscosity adhesive is of benefit. However, the Stephan Equation $Ft=34r2\eta 1H2-\frac{1}{h^2}$ ⧄

(Equation 3) demonstrates that the resistance of the joint to shear stresses is determined largely by the viscosity of the liquid film; a high viscosity is required to create a strong joint.

$$Ft = \frac{3}{4}r^2\eta\left(\frac{1}{H^2} - \frac{1}{h^2}\right)$$ (Equation 3)

In this equation, F is pressure, t is time, r is the radius of the joint, η is the viscosity, and $(\frac{1}{H^2} - \frac{1}{h^2})$ is a term relating the thickness of the joint. Surface tension, viscosity and roughness have competing effects regarding the strength and time for which a bond is effective. As the efficacy of the adhesive depends on both the adhesive and the substrate, both can be modified to create an effective adhesive.

2.2. Adhesive Joint Design

To achieve an effective adhesive joint, several criteria should be met. The adhesive should have good wettability on the substrate, allowing easy spreading and filling of voids. The viscosity of the liquid should be low during application to maximize capillarity and have good wetting, but should solidify to result in an adhesive with high viscosity and resulting strength. The interfaces should be free from contaminant to prevent occlusions. Finally, the surface

9

roughness should be well-designed, avoiding coplanar voids, and modified as to encourage capillary motion.

2.2.1. Wettability

Wettability refers to the extent to which liquids spread over a solid surface, and is related to surface energies (Figure 4).
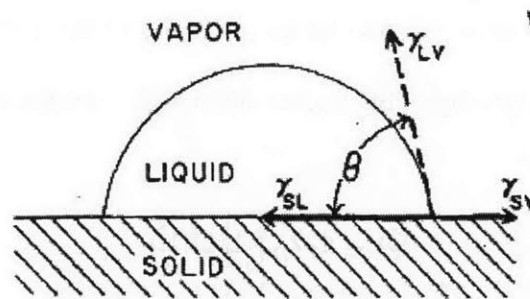
Figure 4. Contact Angle Measurements provide a good indication of surface wettability. Image courtesy of [1].

The surface tension between the liquid, solid, and vapor are a product of the relative surface energies of the different phases present. To allow spreading, the liquid surface energy should be lower than that of the solid, as the liquid spreading will satisfy bonds on the surface of the solid, reducing the total energy of the system. Advantageously, metals have a high surface energy. Good wettability is essential to achieve a uniform coating. Internal stresses and stress concentrations often develop upon solidification of the adhesive, due in part to the difference in the thermal expansion coefficients of the adhesive and the substrate. Poor wetting usually produces a greater stress concentration at the free surface of the adhesive, potentially acting as a source of bond failure.

2.2.2. Coating Uniformity

Drying of the coating is of particular concern due to the solvent evaporation process which may result in a non-uniform coating. A decrease in film thickness at the edge is caused by the

adhesive surface tension. Consequently, the solvent evaporation is much higher at the edge of the film due to a larger surface area per unit volume of fluid near the edge. As more solvent evaporates, the higher surface tension at the edge causes material transport towards the edge (Regon 2 to Region 1 in Figure 5). Newly formed surface in Region 2 has a higher solvent concentration, thus a lower surface tension, causing more material to be transported to the surrounding areas, resulting in non-uniform coatings which may make it difficult to layer the steels. To avoid this phenomenon, the evaporation should be controlled to minimize the flow of material.
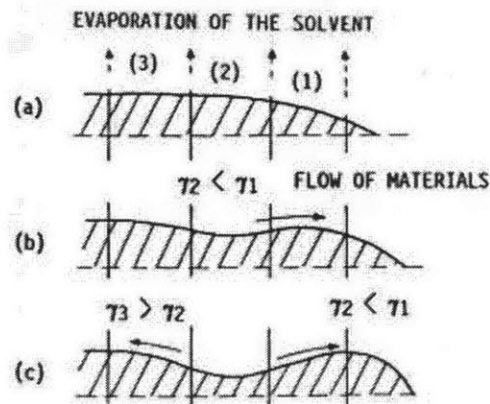
Figure 5. (a) Newly formed film near an edge (b) Flow of materials from region 2 to 1. (c)Further flow of materials from region 2 to the surroundings. Image courtesy of [4].

2.2.3. Solidification to Increase Viscosity

The strength of the joint is proportional to the viscosity of the adhesive (Equation 3), but the viscosity has to be low enough that it can penetrate and fill the capillaries before solidifying. Therefore, a method of solidification that increases the viscosity only after voids have been filled is desirable. There are several means of accomplishing this. The first is solvent removal, in which water evaporates, leaving a much higher viscosity adhesive than was applied. Polymerization, involving a chemical reaction after the adhesive is applied offers an alternative route of accomplishing this increase of viscosity.

11

2.2.4. Pore Minimization

Gas bubbles that form under the layer of adhesive due to viscosity limitations must not be in the same plane when adhering to rough substrates. If these pores are along the same plane, crack propagation from one pocket to the next becomes much more likely, causing the joint to break like an opening zipper (Figure 6).
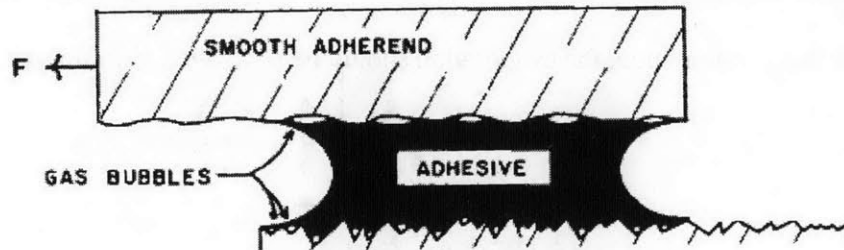
Figure 6. When designing surface roughness into surfaces of adherends, it should be done to minimize the chances of crack propagation. Image courtesy of [1].

To minimize pores, the adhesive should not be viscous upon application and should wet the substrate well, as the higher surface energy of the substrate will pull the liquid adhesive into the pores. Finally, the substrate should be free from contaminants.

2.3. Sodium Silicates

2.3.1. Inorganic Adhesives

Inorganic adhesives have several benefits, including resistance to fire and other chemicals. Due to stronger bonding, they offer the possibility of processing at higher temperatures as they will not melt unlike their organic adhesive counterparts.

2.3.2. Sodium Silicates

As inorganic adhesives, soluble sodium silicates offer several potential advantages, including a very low cost and resistance to combustion. Once the coating dehydrates to the glassy state, it

creates a very stable coating, with an effectively large viscosity. Several mechanical states, from flexible to brittle, can be achieved by curing the firing the adhesives under different conditions. Sodium silicates can be prepared in water, and are available in a wide range of grades, classified by the weight ratios of the silica to the alkali content. Their solubility in water at various concentrations allows control of the viscosity, in turn influencing the wetting and how easily a uniform coating can be formed. The surface energy increases with increased alkali content; the more alkaline the silicate, the greater its wettability. However, at too high alkaline content, the silicates tend to crystallize instead of forming a glass, resulting in inferior coating properties. Therefore, the useful soluble sodium silicates are restricted to a ratio of about 2 to 3.5. [1]

To achieve a good coating, the two parameters considered are the grade, or alkalinity, of the solution, and the concentration of solution in water. The former parameter affects wettability, while the latter affects the viscosity, tailoring it such that it is low enough to be easily applied but high enough to solidify to something of reasonable strength. The concentration of water influences the polarity of the system, further influencing the way the silicate wets a substrate. Figure 7 outlines the ternary system studied in these experiments.
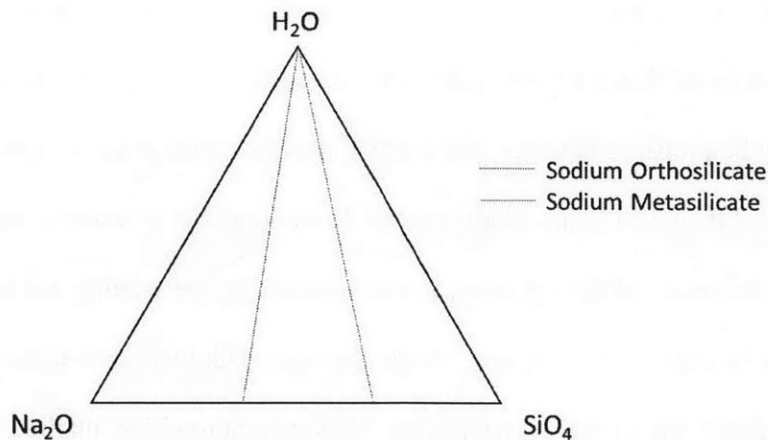
Figure 7. Simplified Ternary Diagram of Na_2O, SiO_4, and H_2O sodium silicate system. Highlighted on the diagram are the phases considered for this experiment, metasilicates and orthosilicates.

The electrical conductivity of the adhesive also depends on the alkali present, as a higher concentration of alkali increases the electrical conductivity. For the ranges of alkali considered, the adhesive still acts as an insulator as required for this application.

As sodium silicates dry by solvent removal, the less water present in the bond, the greater the bond strength, but the more brittle it will be. In applying the adhesive, the percent of water present is used to influence the viscosity, accomplished by altering the processing steps used to reach the desired mechanical properties. The amount of water in the bond has to be dehydrated in a stepwise manner. Complete dehydration only occurs at 550°C. [2]

2.4. Desired properties

For the given application, several properties of the adhesive are of particular importance. It should be non-brittle so it can tolerate the manufacturing processes involved in stamping the metal pieces to the desired shapes. Because the adhesives are used to isolate the layers of electrical steel, the adhesives should be insulating, though this is secondary to the mechanical properties of the joint. Finally, the coatings should be uniform, allowing these properties to extend through the entire structure.

3. Methods

A multi-faceted approach was required to evaluate the efficacy of the sodium silicate coatings. The coatings were assessed on two main criteria: coating uniformity and quality, and mechanical properties.

3.1. Coating Wetting and Uniformity

Application of a uniform, thin film coating of the sodium silicate to the electrical steel was requisite for the insulating layers. To permit uniformity, the solution needed good wettability and to have adequately low viscosity.

3.1.1. Wetting

The wetting of the solution on the substrate was quantified through sessile drop contact angle measurements. A constant volume of the adhesive in solution was dropped on the substrate from a fixed height (Figure 8). Five drops were made per substrate, and five coupons of each substrate were tested for each solution. Using a HIROX digital microscope, the profile of the drops on the substrates was recorded and the contact angles between the adhesive and the substrate were measured to relate surface energies.
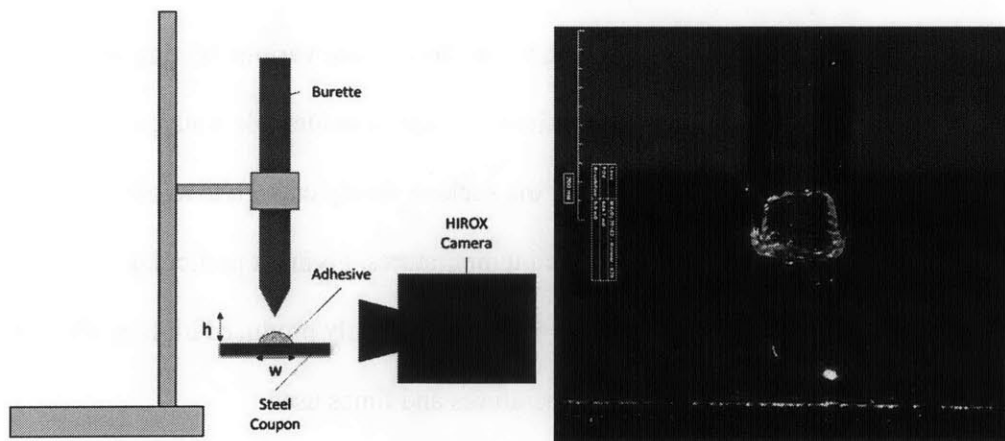

Figure 8. (Left) Contact Angle Measurement Experimental Setup. (Right) Burette was positioned 4mm above the substrate and dropped a constant volume of liquid on the surface

15

3.1.2. Coating Application

The coatings were applied using a Mayer rod coater. The coating thickness was controlled by the area of the grooves between coils of wire (Figure 9) and the speed of application. A small pool of the coating solution was deposited ahead of the rod and the moving rod leveled the material to produce a smooth, uniform thickness coating on the coupon. Between coatings, the rods were cleaned to avoid solution solidification in the grooves. All coatings were prepared at the lowest coating speed, rolling the rod over the substrate twice to ensure uniformity.

WIRE WOUND ROD

wire coils   rod

adhesive   substrate to be coated
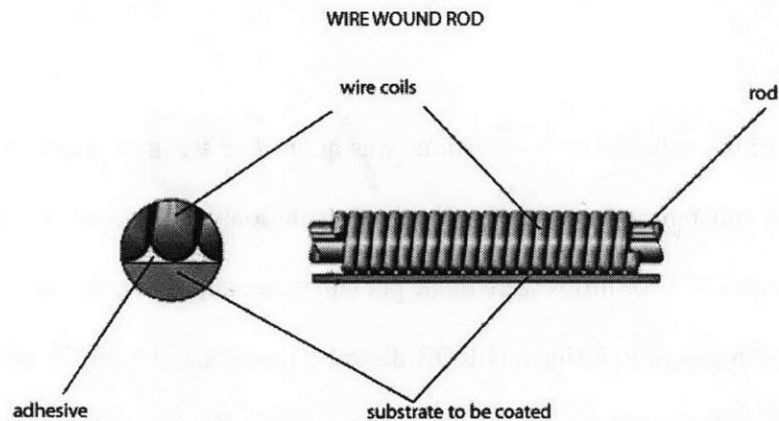
Figure 9. Mayer Rod Coater. The gauge of the wound wire controls the thickness of the applied adhesive. Image courtesy of [3].

3.2. Processing Parameters

Once a uniform liquid coating was applied, it was dried using various heating profiles to result in a clear, uniform coating. As the adhesives contains considerable water, a step-wise profile was required to evaporate the water off the surface slowly enough to avoid boiling. Once the coating was dried, it was fired at an elevated temperatures, giving it particular mechanical properties. Figure 10 outlines the drying process that consistently produced high quality dried adhesives, while Table 1 details the firing temperatures and times used.
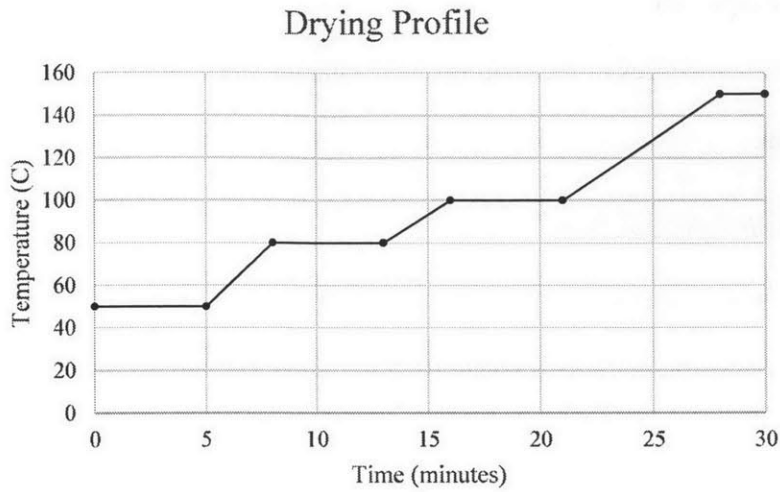
Figure 10. Step-wise drying profile for uniform coating

Table 1. Firing Parameters for Coating Preparation

Firing Temperature (°C)	Firing Time (minutes)
500	5, 10, 30
600	5, 10, 30
700	5, 10, 30
800	5, 10, 30
900	5, 10, 30

3.2.1. Verification of Uniformity

The uniformity of the substrates was determined via two methods. Visual observations of the substrate immediately after both applying and drying the coating were made to verify that obvious adhesive concentrations had not formed, either as pools, uncoated portions of the substrate, or noticeable material lacking from the edges at outlined in 2.2.2. Cross sections of the coatings were measured using the HIROX to evaluate coating uniformity across the substrate.

3.3. Mechanical Properties

The mechanical properties of the coatings were characterized by their adhesion and resistance to strain.

3.3.1. Cross Hatch Adhesion Tests

The adhesion was measured by tape tests according to ASTM D3359 using an Elcometer Cross Hatch Cutter. Six parallel blades were used to cut the coating, followed by an additional six cuts made at ninety degrees to the original cuts. Adhesive tape was smoothed over the grid, ensuring good contact with the film, then rapidly removed. The grid was inspected visually, the number of flaked squares counted, and the adhesion was rated according to (Figure 11) and percentage of squares removed.
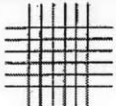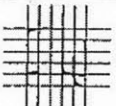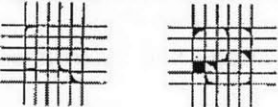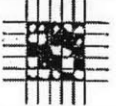
CLASSIFICATION	PERCENT AREA REMOVED	SURFACE OF CROSS-CUT AREA FROM WHICH FLAKING HAS OCCURRED FOR SIX PARALLEL CUTS AND ADHESION RANGE BY PERCENT	
5B	0% None		
4B	Less than 5%		
3B	5 - 15%		
2B	15 - 35%		
1B	35 - 65%		
0B	Greater than 65%		

Figure 11. Cross-Hatch Test Visual Quality Test as per ASTM D3359. Image courtesy of [4]

3.3.2. Mandrel Tests

The elongation of the adhesive coating was tested by a cylindrical mandrel bend test in accordance with a modification of ASTM D522 for inorganic coatings [5]. In this qualitative test, coupons were clamped onto the test equipment and the test pieces were bent over decreasing mandrel radii until the coating cracked or flaked off. The mandrel diameter at which the coating failed was correlated to a strain, and strain thresholds for the coatings were determined.
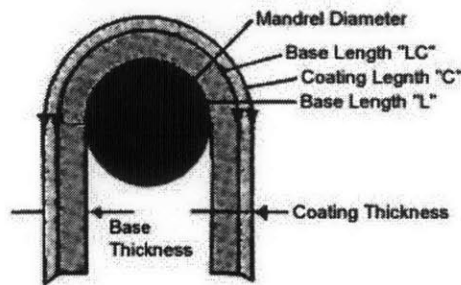
Figure 12. Mandrel Test to determine resistance to strain. Image courtesy of [6].

3.3.3. Three-Point Bending Tests

Three-point bending tests performed as a modification of ASTM C1161 were used to quantify the adhesion and flexibility of the coatings (Figure 13) [7]. Similar to the mandrel tests, the substrate was strained and the response of the adhesive was recorded. From the stress-strain curves, a precise failure strain could be determined. Further analysis of the curves provided a depiction of the cracking evolution as increased noise corresponded to releases in stress by microcracks in the coatings, though these cracks did not result in failure.
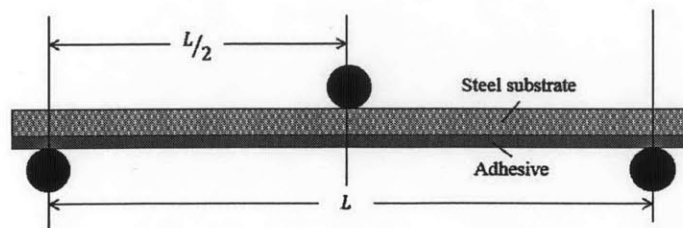
Figure 13. Three-point bending test setup to determine flexural strain. The strain is correlated to the maximum deflection.

3.4. Description of Systems Tested

Table 2 summarizes the adhesives and substrates considered to evaluate the inorganic coatings.

Table 2. Adhesives and Substrates considered for testing

Adhesives	Substrates
10wt% Sodium Orthosilicate	POSCO Low Grade Electrical Steel, Roll Direction
20wt% Sodium Orthosilicate	POSCO Low Grade Electrical Steel, Cross Direction
37.5wt% Sodium Orthosilicate	POSCO High Grade Electrical Steel, Roll Direction
10wt% Sodium Metasilicate	POSCO High Grade Electrical Steel, Cross Direction
20wt% Sodium Metasilicate	Glass
44wt% Sodium Metasilicate	
Water	

The compositions of the sodium orthosilicates and sodium metasilicates were limited by solubility in water, 37.5 wt% and 44 wt% respectively [8]. The contact angles for water on glass substrates have been well characterized [9]; this was used as a standard to verify consistency of the method. High and low grade electrical steels were tested, differentiated by their relative silicon composition: the high grade contains 2 wt% Si, while the low grade contains 0.7 wt% Si. The presence of silicon increases the electrical resistivity of the steel, reducing the core loss, but embrittling the material, particularly following the cold-rolling process used to produce the electrical steel. The resulting anisotropic grain structure as well as the changed surface chemistry influences wettability. It was anticipated that the surface roughness in the direction of the rolling would differ from that in the cross direction due to the resulting grain structure.

4. Results and Analysis

4.1. Contact Angle Measurements

The contact angles of the adhesive of various concentrations on different electrical steels was characterized based on alkalinity of the adhesive and chemistry and anisotropy of the substrates. The measured contact angles were normalized over average surface roughness measurements as determined through surface profiles collected on the HIROX.
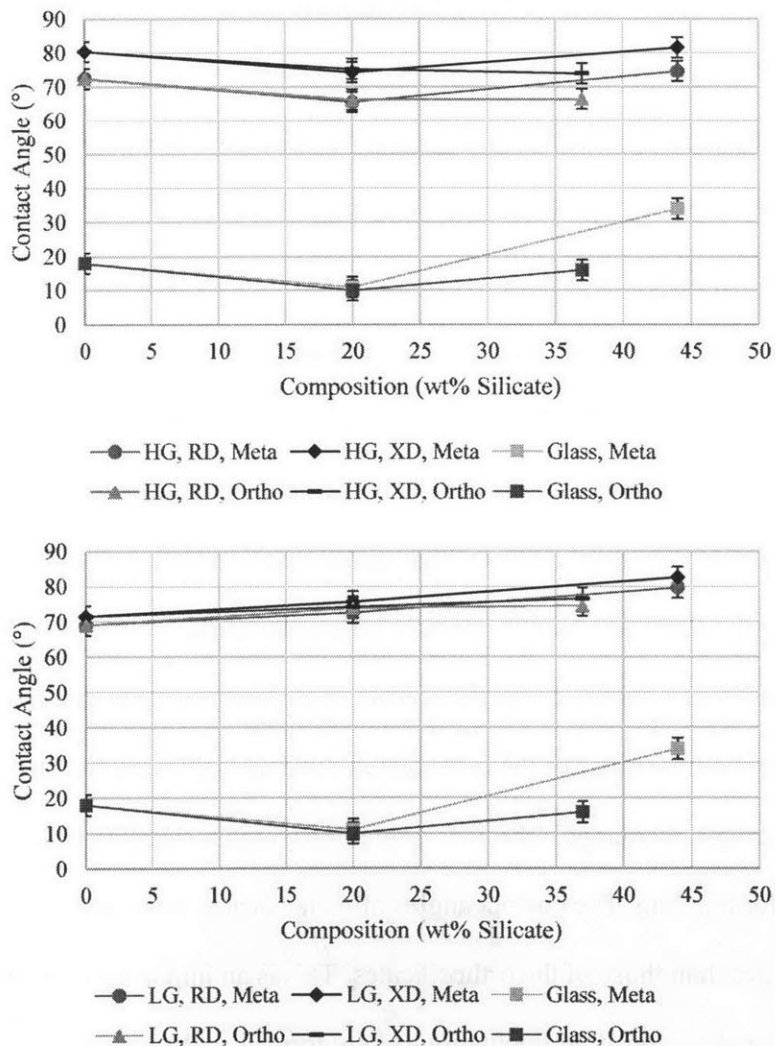

Figure 14. Contact Angles Measurements as a function of composition on different steels. Top: high grade electrical steel. Bottom: low grade electrical steel. HG and LG refer to High and Low Grade Steel. XD and RD refer to roll and cross direction.

4.1.1. Degree of Alkalinity

Orthosilicates and metasilicates differ in their relative compositions (2.3.2); orthosilicates have a higher concentration of SiO_4 whereas metasilicates have a greater concentration of Na_2O. The composition difference affects the number of groups available to bond to the surface of the electrical steel. Increased alkali content generally increases the surface energy of the adhesive, making bonding more favorable. The presence of active groups on the surface of the steel, including silicon and oxygen, offer bonding locations for the active groups of the adhesive.

The ratios of Na_2O and SiO_2 were constant for the silicates tested; various proportions of water were tested for each ratio. By changing the concentration of water present, the viscosity of the adhesive and the active groups present to bond with the surface varied, as higher concentrations of hydrogen and oxygen were available with increased water content. At low silicate concentrations, the orthosilicates and metasilicates exhibited similar contact angles on the examined substrates Figure 14. Pure water exhibits low wettability on these surfaces because the hydrogen bonds make it energetically favorable to maintain the polar bonds within the water droplet. Water is highly cohesive and has a high surface tension [10], so bonding with the surface is energetically costly; the water droplet contacts little of the surface. To an extent, increased proportions of Na_2O and SiO_4 decreased the contact angle because these constituents encourage adhesion. At higher compositions of the orthosilicates and metasilicates, the large concentrations of the functional groups encourage cohesion. Achieving a high wettability occurs by balancing groups available for bonding. The contact angles of metasilicates were more sensitive to composition changes than those of the orthosilicates. This is an important consideration in design of the system, as local composition fluctuations likely formed as the coating dried, resulting in uneven wetting. For all accessible compositions, the wetting properties were not remarkable and

did not exhibit large variability; reaching a minimum contact angle between 30° and 40° around 80 wt% H_2O for both silicates tested.

4.1.2. Surface Morphology Effects

The orthosilicates and metasilicates demonstrated similar contact angles for the high and low grade electrical steels (Figure 14). The grades of steel are differentiated by their composition; the high grade contains over twice the silicon of the low grade steel. The higher silicon presence was anticipated to increase the wettability of the adhesives; the silicates contain SiO_2 bonds, which could easily form bonds with the excess silicon on the surface.

Contact angles on the low grade electrical steel were observed to be slightly lower than on the high grade electrical steel for all compositions tested, as anticipated based on the higher degree of silicon present in the chemistry of the surface. However, the difference in the mean contact angles was not large enough to be statistically significant as determined by pairwise t-tests (p-value > 0.05) due to the limitations of the measurement technique. Therefore, the greater silicon presence did not have enough influence to substantially change the surface chemistry and wettability.

A second difference between the high and low grade electrical steel was surface microstructure. Because the silicon presence affects the mechanical properties, the surfaces of these metals after processing vary. In both steels, the cold rolling process results in an anisotropic surface. While the resulting grains were similar in size, the high grade electrical steel was more brittle and had more pronounced surface roughness due to this process (Figure 15).
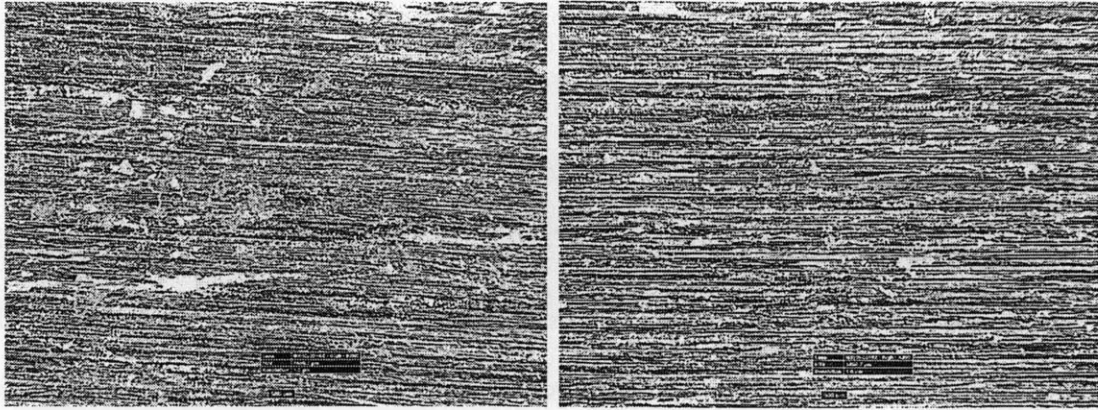
Figure 15. High grade electrical steel (left) and low grade electrical steel (right). Both steels are have anisotropic surfaces. Microstructural differences between the two result from different mechanical properties of the steels. 200x magnification.

For all compositions considered, the contact angle was much higher on the metal than on the glass. The larger contact angles can be attributed to decreased relative surface energy and increased surface roughness. Lower surface energy decreased the wettability because it was less favorable for the adhesive to spread. This was a product of the groups available on the surface for bonding: the glass is also sodium silicate, so it is favorable to form bonds with the adhesive, whereas on the steel, it is therefore less favorable to create a surface-adhesive interface (Figure 16).

Figure 16. The solutions were much more wettable on the glass (left) than on the steel (right) due to surface energy and microstructural differences.

24

As a result of the rolling, the metal has a clear anisotropic microstructure (Figure 15) and associated roughness. In the roll direction on the high grade electrical steel, the contact angles were consistently 5-10% smaller than in the cross direction because the crevices are on a length scale comparable to the size of the drops, whereas in the cross direction, a d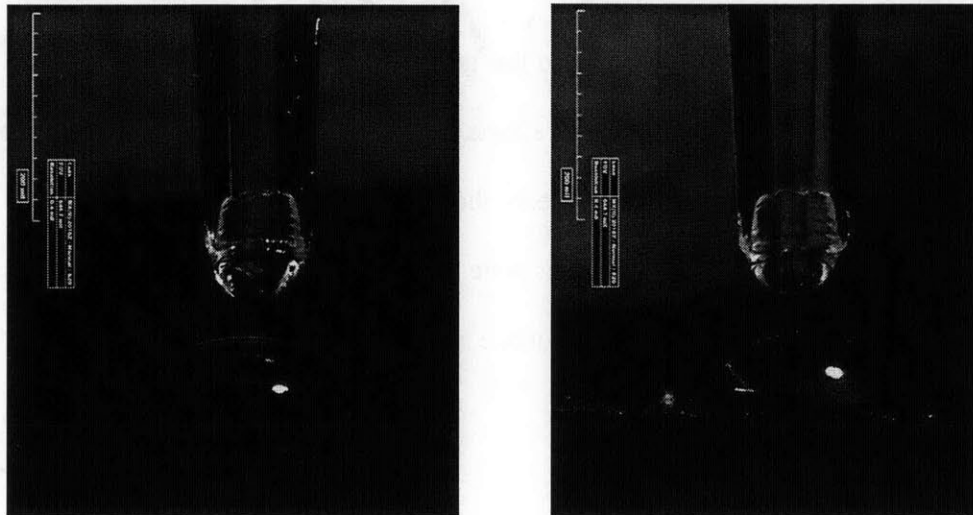rop spans several crevices. For the low grade electrical steel, this contact angle anisotropy was not observed, reiterating the point that the added silicon results in microstructural differences.

The contact angles were normalized to account for the surface over which they were spread. When the grains or surface asperities occur on the same length scale as the size of the drops, the surface behaves ideally, as a smooth surface. In the cross direction the surface cannot be assumed to be ideal because the surface is rougher. Because the contact angle is less than 90°, it was assumed that the wetting occurs according to the Wenzel wetting model [11]. In this model, the drop penetrates the pores and the contact angle appears higher than the actual angle according to the equation

$$\cos \theta^* = r \cos \theta \qquad \text{(Equation 4)}$$

where θ^* is the apparent contact angle, r is the surface roughness, and θ is the actual contact angle. This equation accounts for the additional interface that is being accommodated by the drop by measuring surface roughness, the vertical deviations of a surface from its ideal, smooth form.

Rougher surfaces are generally more hydrophobic than smooth surfaces. It was assumed that Wenzel wetting was occurring but it is possible that some air pockets were caught in the voids instead of filling completely – a reasonable assumption based on the adhesive viscosity. This is known as the Cassie-Baxter model [11], and reduces wettability because air-adhesive interface is

made instead of adhesive-substrate interface. The actual wetting state observed was likely

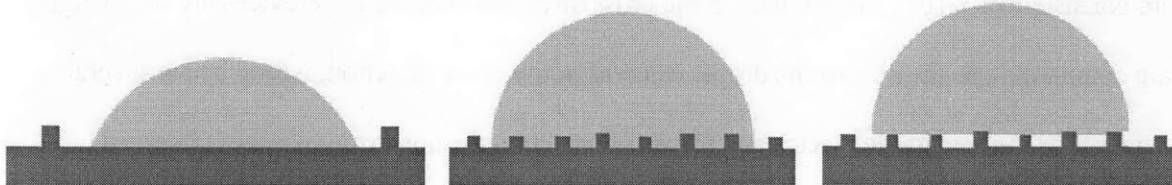between the two extremes of the Wenzel and Cassie-Baxter models.

Figure 17. Wetting in the roll direction (left) and the cross direction (right). On the rougher surface, the drop has increased surface area contact, increasing the apparent contact angle (Wenzel wetting). If air pockets form in the surface asperities, the contact angle increases (Cassie-Baxter wetting).

4.1.3. Relative Surface Energies

The sodium orthosilicates exhibit a weaker contact angle dependence on the composition

than the orthosilicates. This may prove advantageous due to inhomogeneities in the solution as

well as those that may arise in the drying process: if the wettability is not heavily dependent on

the composition, larger room for error as may be seen under large-scale processing conditions

would be favorable.

The wettability of the adhesive does exhibit some extent of anisotropy on the rough surfaces.

The anisotropy was not pronounced and should be not a large concern industrially.

Based on contact angle measurements alone, the compositions which minimize the contact angle

would be best for the application, but other criteria were also considered. A low contact angle

was important to allow filling of the crevices and homogeneous spreading over the surface. To

facilitate this, the viscosity must be low but the water content cannot be so high that the

evaporation leaves little sodium silicate; adequate sodium silicate is required to insulate the steel.

Contact angle measurements indicated wettability limitations, but the worth of varying adhesive

concentrations were analyzed based on several criteria.

4.1.4. Analysis of Sessile Drop Method

To test the validity of this method, including confirmation of the constant volume and distance over which the adhesive was dropped, the system was calibrated using a water drop on glass. At a height of 4mm and the drop volume tested, contact angles similar to literature values were measured. The drop height was limited by the volume required to form a drop; the lower the burette height, the less the drop deformed upon impact with the surface, but adequate area to form the drop was required.

Due to the cold rolling process, many of the steel coupons had surface features including scratches, oxidation, and contamination (Figure 18). Although the surfaces were cleaned with ethanol immediately prior to testing, some surface features remained and may have affected the wettability of a particular area. The variance in substrate quality accurately represents a potential concern for industrial use of these adhesives: the manufacturing process must account for surface inhomogeneities. For analysis purposes, the variance was minimized by testing several coupons to account for an average number of surface features.
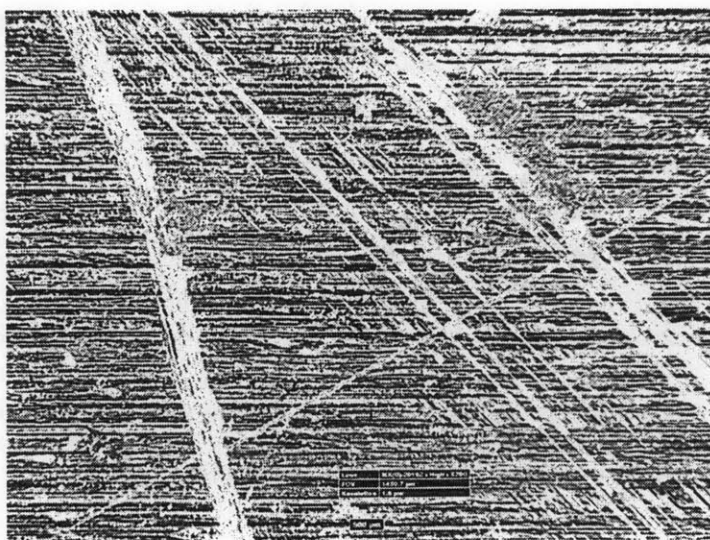

Figure 18. Surface exhibiting scratches and oxidation in addition to microstructure left by rolling process. 200x magnification.

The methods of contact angle measurement have several limitations, particularly for rough surfaces. Though the camera was tilted to allow the substrate to be reflected by the drop, more easily differentiating the interface, the interface between the drop and substrate is not clear due to surface roughness. It has often been seen that the measured contact angle is higher than actual contact angle [12], leading to a systematic under estimation of the interface energy. A further systematic error is the dependence of the contact angle on the volume of the droplet. Nonetheless, contact angle measurement methods prove useful in considering relative surface energies.

Reproducibility of the method was limited because the accuracy of contact angle measurements depended on the assignment of the tangent line. There was some ambiguity about where on the drop to measure the angle, changing the recorded angle by up to eight percent (Figure 19). To maximize accuracy, the author considered the steepest tangent line to calculate the contact angle. Several measurements of the drops were taken to calculate the error associated with this method.
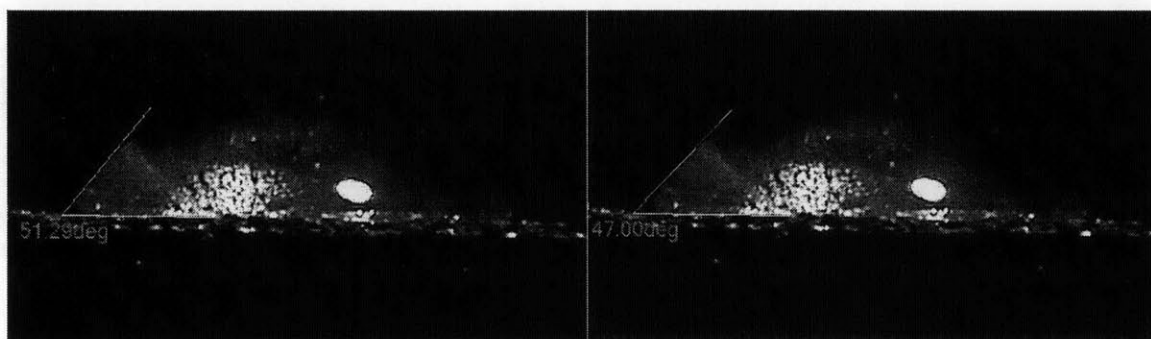

Figure 19. A substantial difficulty associated with the sessile drop method is the determination of the tangent line. Large variation can be found in the contact angle based on selected tangent. The fit pictured on left was used for all the measurements in this experiment.

4.2. Microstructure and adhesion

Once a uniform coating had been applied to the substrates and dried, the adhesives were fired at elevated temperatures, resulting in altered mechanical properties. The firing temperatures and times influenced the microstructure of the adhesive, relating to the modes by which they failed in mechanical testing. The coupons were heat treated between 500°C and 900°C. Cross-sectional coupons were observed under the HIROX microscope and the thickness of the adhesive layer measured to ensure a uniform coating.
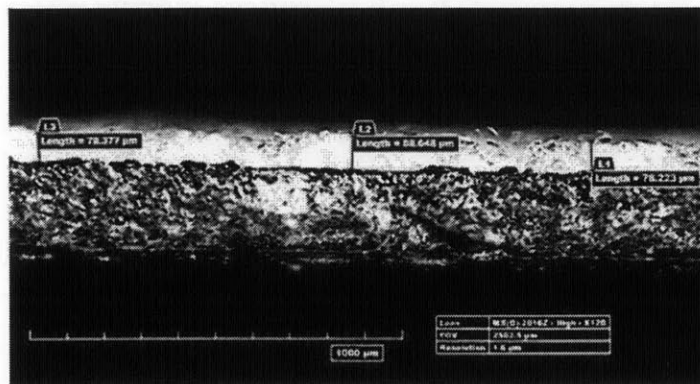

Figure 20. Process used to measure the thickness of the adhesive on the substrate

Figure 21 shows the adhesive thickness as a function of processing temperature. Increased firing temperatures resulted in decreasing coating thickness. At very high firing temperatures, the adhesive completely evaporated, leaving only an oxide layer on the surface.
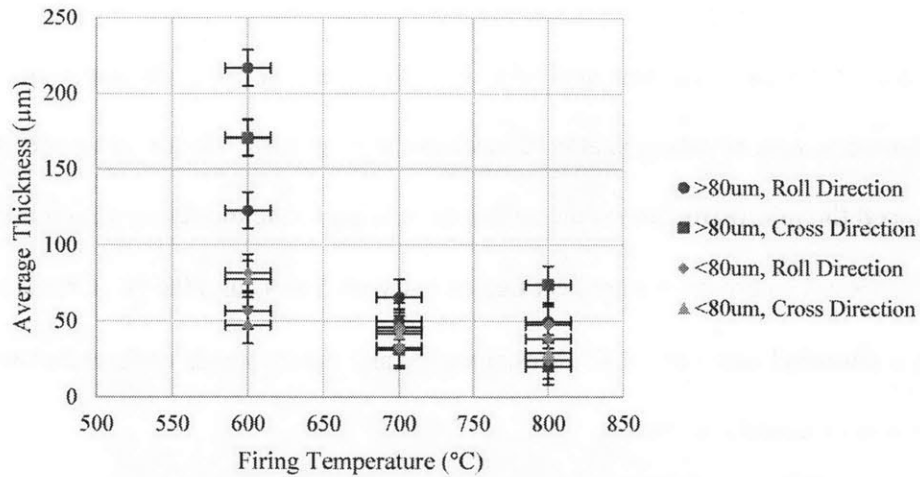
Figure 21. Thickness as a function of firing temperature

The adhesive thickness in the cross direction did not vary largely from that in the roll direction (p-value = 0.49); this speaks to the quality of the adhesive application despite differences in wettability. As local curvatures increase the chemical potential of the surface, the minimum chemical potential was achieved by creating a uniform coating. [13]

Due to chemical potential differences at the edges, there were concerns about the coating thickness near the edges (2.2.2). Figure 22 compares coating thickness taken at the edge to that away from the edge. No appreciable differences in the average film thickness were observed, though the thickness at the edge had a higher variance. The increased variance indicates a difficulty in controlling the edge thickness, but this was limited to within several millimeters from the edge.
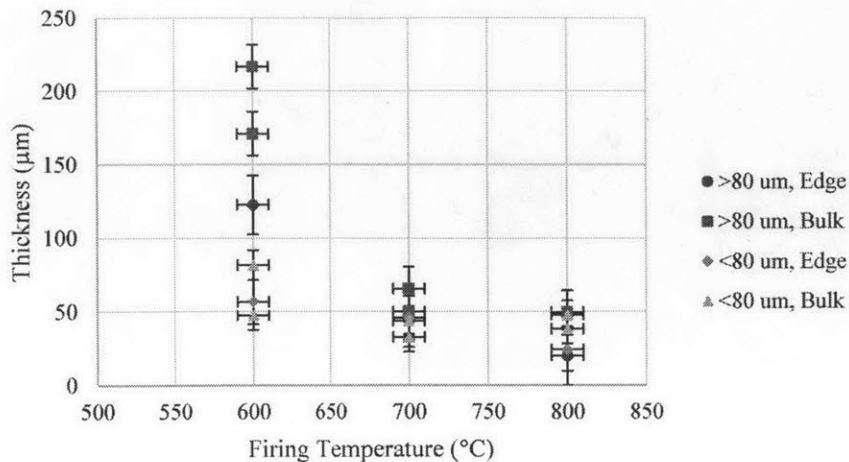
Figure 22. Adhesive thickness at edge compared to the bulk

The average thickness for each firing temperature are summarized in Figure 21. This measurement only takes into account areas in which the coating was present; many of these coatings had certain spots on the surface with gaps in the coating. Although the coatings were macroscopically uniform, microscopic variations could be observed across the surface (Figure 23-25).

The lowest and highest firing temperatures resulted in ineffective coatings for all orthosilicates and metasilicates tested. Fired at 500°C, the water evaporated off the surface at a rate that allowed the water vapor to form pockets within the adhesive layer. These expanded and popped, resulting in a thick, flaky coating with large voids (Figure 23).
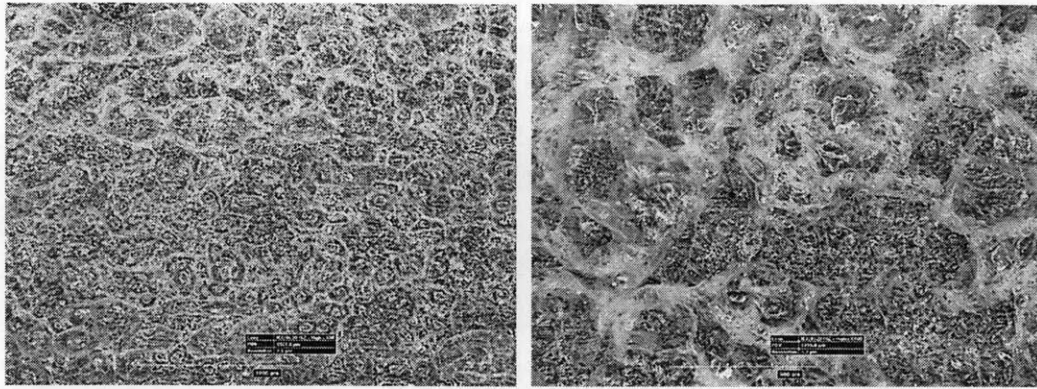
Figure 23. Sodium Orthosilicate fired at 500C exhibits large pockets from water vapor. Left: 80x magnification. Right: 160x magnification.

At the maximal processing temperature, 900°C, the adhesive burned off the surface, leaving only an oxide coating. Thus, an operability limit was determined. Firing temperatures within this range are thus required such that any water left after drying the substrate could evaporate to avoid forming large vapor pockets, while not burning the adhesive off the surface. The microstructure of the coupons fired in the range of 500°C to 900°C are shown in Figure 24-25.

Figure 24. Sodium orthosilicate fired at 700C still exhibits some pockets, though they are less pronounced than those at 500C. Left: 80x magnification. R: 200x magnification.
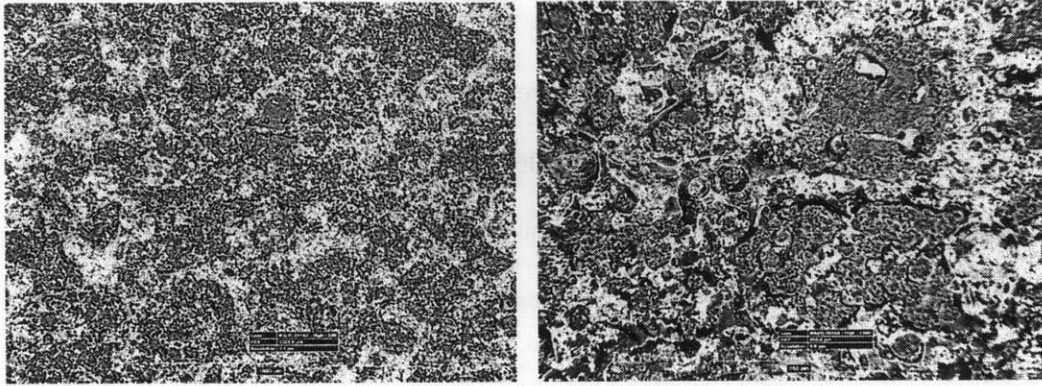
Figure 25. Sodium orthosilicate fired at 800C does not cover the surface homogeneously, but has no pockets as observed at lower firing temperatures. Left: 80x magnification. Right: 160x magnification.

For all firing temperatures, the adhesive was considered to coat the substrate well as none of
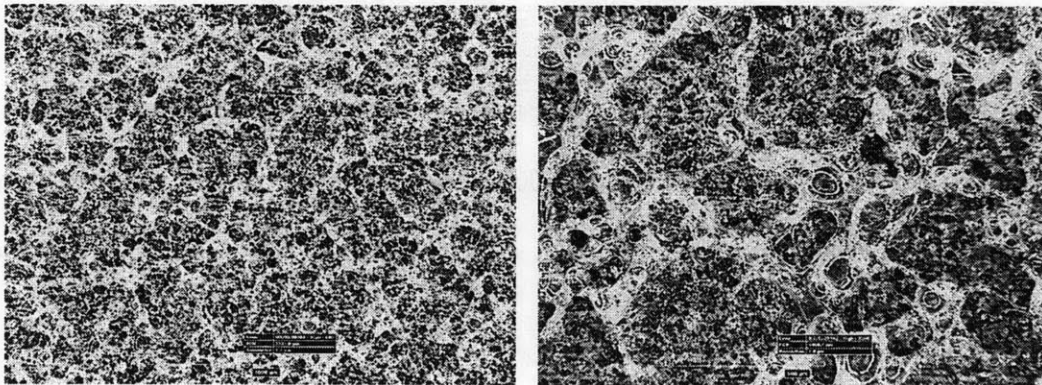
the original steel microstructure can be seen, although there are obvious regions of higher and

lower adhesive concentration. The voids in the adhesive surface result from the original solution

not being completely homogeneous and water evaporation occurring at uneven rates.

Once fired, the adhesive properties of these were tested via the cross cut tape method as outlined

in 3.3.1.

Figure 26. Coating removed via the adhesion tape test as a function of firing temperature. The metasilicates experience significant loss for all temperatures tested. The orthosilicates have improved adhesive with higher firing temperatures.

This method is qualitative in its execution and in the results it yields, so the adhesion was tested via further methods (3.3.2 and 3.3.3). However, the test does yield informative results. As can be seen, the metasilicates lose significant material once fired at an elevated temperature, suggesti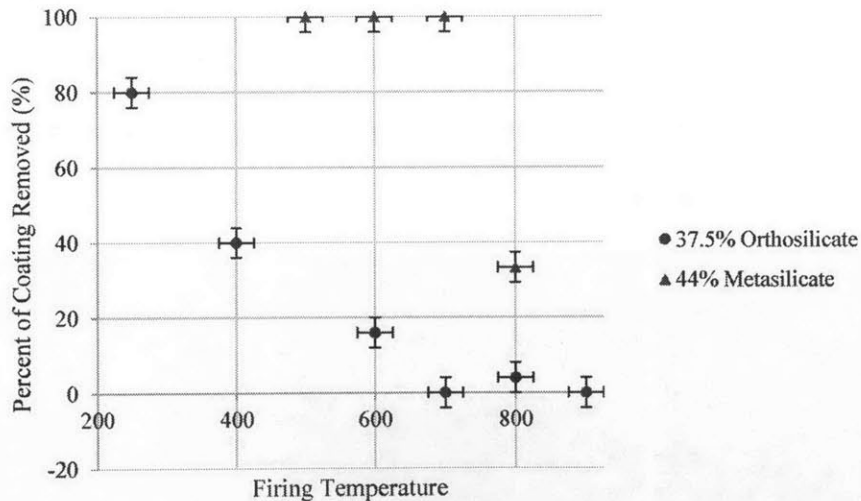ng that the adhesion is inadequate. For the orthosilicates, as the firing temperature increased, the amount of coating removed decreased significantly, as fewer flakes resulting from water evaporation were removed.
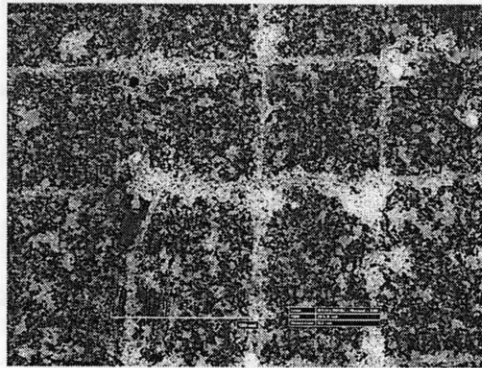
Figure 27. Adhesive tape with coating adhered to it after the cross hatch test. This amount of material is indicative of poor adhesion.

While the majority of the tests considered different firing temperatures, the influence of firing time on the resulting microstructure was also measured. Firing at a constant temperature, 700°C, the coupons were fired for 5, 10, and 20 minutes various firing times were tested; the resulting microstructures were observed.
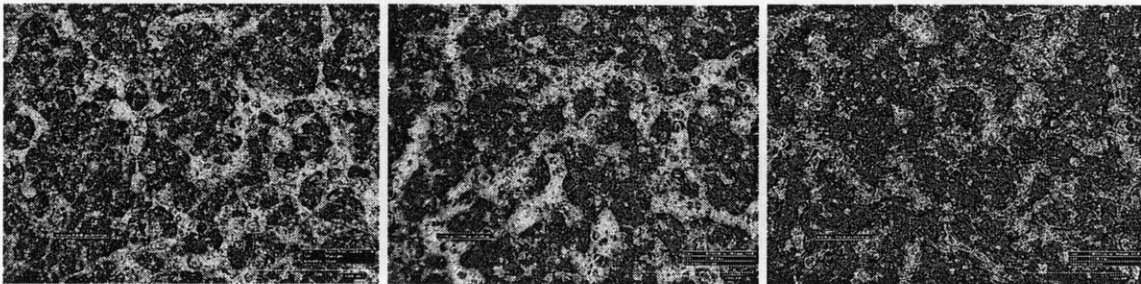
Figure 28. From left to right: Substrates with adhesive after firing at 700C for 5, 10, and 20 minutes. 100x magnification.

From the micrographs, it can be seen that at longer times at elevated temperatures, reduced

adhesive remains on the substrate. As the water content of these adhesives is quite high, there is

significant evaporation contributing to the loss of adhesive. The microstructure of the remaining

adhesive does not change with increased firing time, as the size and distribution of bubbles

within the adhesive remains constant. Therefore, it was concluded that the temperature was

largely responsible for the mechanical properties of the coating. No further changes in adhesive

coverage were seen with firing times greater than twenty minutes.

4.3. Mechanical Tests

As the coated steel pieces will be bent as they are machined, resistance to strain of the

underlying material is imperative. When the material bends, the adhesive mist remain affixed to

it to be effective. Several potential failure mechanisms, including flaking off the surface, brittle

fracture, and loss of adhesion were considered in the analysis of mechanical properties using two

methods

4.3.1. Mandrel Tests

Mandrel tests provided good evidence for thresholds which could be reached by the materials

under consideration, as failure strains were determined by bending coupons around mandrels of

decreasing diameters.

4.3.1.1.   Flexural Strain Thresholds

The samples were bent over the mandrels both immediately after drying and after firing; the

failure strains are summarized in Figure 29. The bend tests after drying were used to determine

the drying profile as outlined in 3.2.
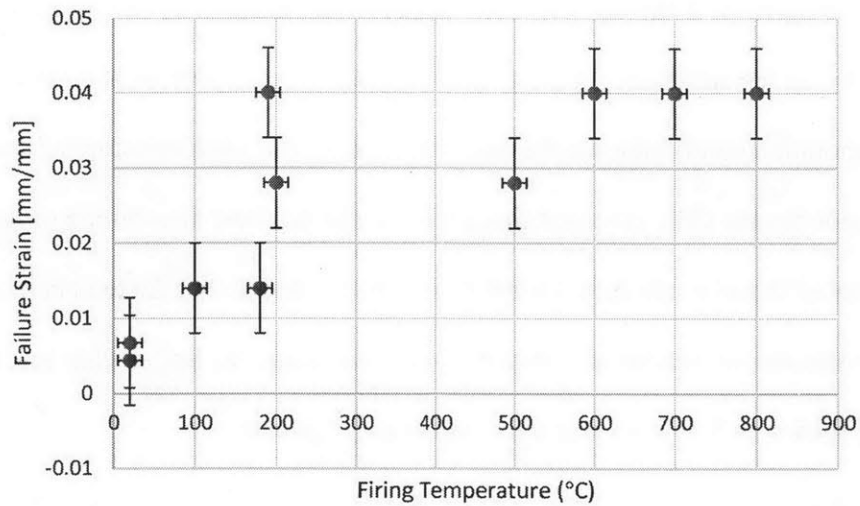
Figure 29. Failure strains resulting from the mandrel tests.

The strains were calculated via the ASTM standard D522. All of the failure strains marked as 0.04 mm/mm correspond to the limit of the mandrels: after being bent over the smallest mandrel, the coating had not failed, so all threshold strains were ranked equally. The large error associated with these measurements is a result of large changes in strain between the mandrels around which the coupons were bent.

4.3.1.2. Mandrel Test Analysis

An important limitation of this mandrel test method was imprecision at high strains. Once the processing conditions were improved to the point where the adhesive had some flexibility and did not readily undergo brittle fracture, the method had restricted usefulness. The method was thus useful at differentiating between very poor coatings and better coatings, but could not distinguish between better coatings because only certain strains could be tested. Furthermore, the testing method tests discrete strain values, the set diameters of the rods around which the coupons are being bent. The mandrel tests only give the bounds of failure and more rigorous testing is required to determine the actual failure strain.

A final significant limitation of this testing method was the application of localized stress. As the coupon was bent around the rod, the maximum stress was applied along one line on the material. Given the potential presence of localized surface features or defects, the test may have failed at a strain not representative of the entire surface. This limitation was mitigated by testing several lines on the surface to statistically reduce this error.

4.3.2. Three-Point Bending Tests

Three-point bending tests were performed on the coupons to overcome several of the limitations associated with the mandrel test. In particular, this method offered the ability to test continuous values of strain and to find a precise failure strain.

4.3.2.1. Stress-Strain Analysis of Three-Point Bending Tests
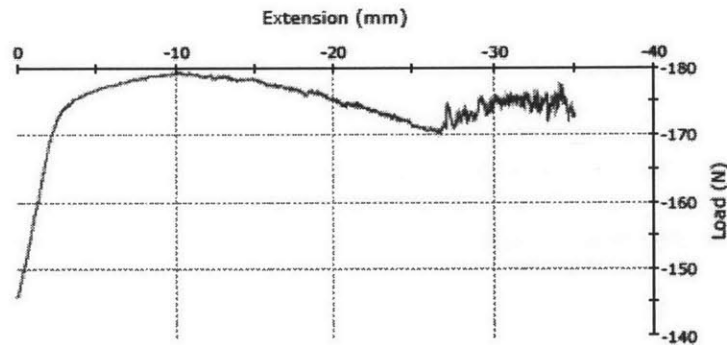
Figure 30. Stress-Strain curve for coupon fired at 700C. The onset of noise is quite apparent.

Because coupons failed via various mechanisms, the strain at which they failed was difficult to discern. For example, those adhesives which failed due to cracks that have developed in the straining process have the small cracks developing over a range of strains. As a comparison, those which have failed via a brittle failure mechanism exhibit a sharp change in the stress strain curve, which could be considered the point of failure, but have also been undergoing microcracks for a range of stresses. Thus, for comparison purposes, the onset of noise within the stress-strain

curves, which corresponds to the onset of the cracking of the surface structure, was taken to be

an indication of the rest of the failure stress. This "onset strain" is plotted as a function of firing

temperature in Figure 31.
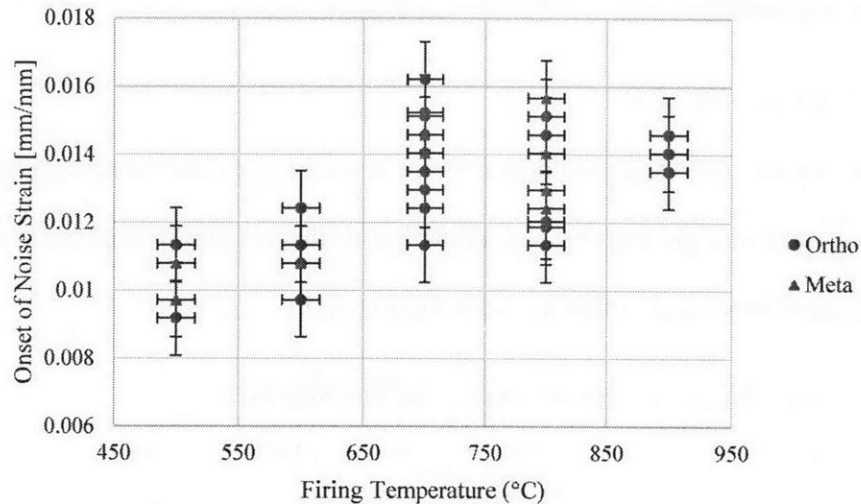
Figure 31. Onset of noise, thus cracking, as a function of firing temperature from three-point bending tests.

It can be see that the onset of noise happens at the highest strain for the adhesives fired

between 700°C and 800°C, though there is significant variance in the onset strain for coupons at

each of the firing temperatures.

4.3.2.2. *Three-point Bending Test Analysis*

The three-point bending tests were subject to the same major limitation that arises from

localized load application: the strain is highest along the line on which it is loaded, so failure was

most likely to occur along this line. Again, several tests were made of a given sample to reduce

statistical variation. A four point bending test would test a larger area, offering a means to

overcome this if more thorough testing were required. However, the microstructure of the

coating was observed to be moderately homogeneous across the surface, so it was assumed that this was not a significant limitation in this application.

A second limitation that arose was restricted testable strains due to the geometry of the test setup. As the test coupons were only available at a certain maximum length, the maximum deflection of the coupon was limited by what could be balanced by the test equipment. For some of the coupons, this deflection was not significant enough to result in failure. As this strain is large enough to result in plastic deformation of the steel, it was assumed that the coating would satisfy a sufficient threshold for the required mechanical properties.

4.3.3. Failure modes

Many different failure mechanisms were observed after the bending tests. While some of the coatings exhibited brittle fracture upon being strained, several other failure mechanisms were observed relating to the coating adhesion and the development of microcracks to relieve strain.
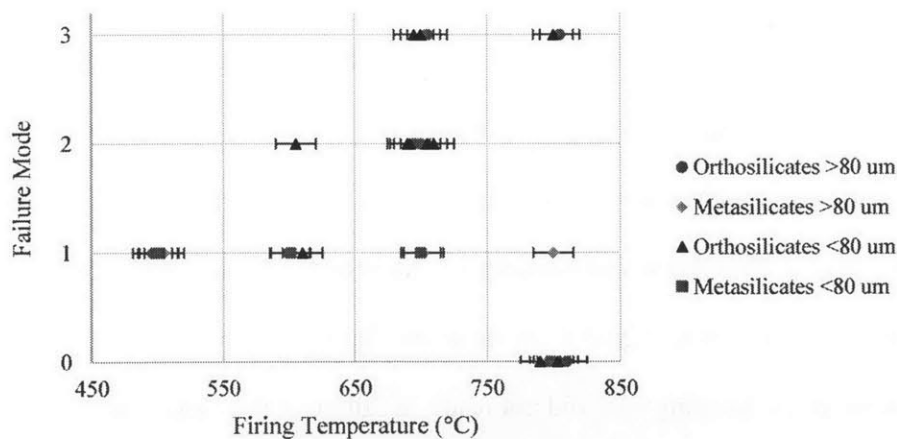

Figure 32. Failure modes observed at varying firing temperatures. 0: no failure, 1: adhesion failure, 2: flaking due to microcracks, 3: brittle failure

For the metasilicates, the coating could be removed after straining by simply applying a light shear force, accomplished by brushing a finger across the surface. Portions of the coatings on the

centimeter scale were removed with this, indicating a failure in the adhesion of the coating: rather than the mechanical properties of the coating being the limiting factor, their adhesion to the substrate failed. This failure, coded as "Type 1" in Figure 32, was considered an adhesion failure. Metasilicate adhesives fired at all temperatures underwent this failure mode, reflecting the results of the tape adhesion test. This failure mode was also observed for low firing temperatures (500°C to 600°C) for orthosilicates.

At higher processing temperatures (500°C to 700°C), the failure mode was dominated by a flaking of the coating upon the application of a shear force. These flakes were significantly smaller than the mode described above, suggesting a failure mode due to a change in the coating. As the coating was strained, the interconnected structure of the adhesive broke to accommodate the strain, reflected in fluctuations in the stress-strain curves and popping sounds observed during the tests. These microcracks were able to relieve strain locally without compromising the overall structure of the coating unless a shear force was applied. This failure mode is coded at "Type 2" in the above figure.

The highest processing temperatures resulting in a successful coating (700°C to 800°C) exhibited brittle failure. This failure occurred at the loading point. Complete disruption of the adhesive structure was required to accommodate the strain. Once this occurred, the coating peeled off the surface. This mode was considered a mechanical failure of the coating which led to an adhesive failure, coded as "Type 3" in the above figure.

Finally, some of the bending tests did not result in failure of the coating within the tested regime ("Type 0"). This occurred for the thin coatings fired at relatively higher temperatures (700°C to 800°C).

5. Discussion and Conclusions

5.1. Discussion: Sodium Silicates as Adhesives

The efficacy of the adhesives depended on properties of the adhesive material, the substrate onto which they were applied, and the interaction of the coating and substrate, making the task of evaluating the usefulness a complicated one, as made apparent from the variety of tests and conclusions drawn from those. By focusing on the key requirements of the systems in which these steel-adhesive stacks are to be used, it was possible to hone in on the most important properties to characterize these adhesives. Namely, adequate adhesion even under applied loads and high temperatures were required to maintain an electrically insulating bond between steel layers for mechanical and electrical stability. The ability of the adhesives to accomplish this was measured via several methods, with some key results.

1. Sodium silicates with increased alkali content (i.e. the orthosilicates) exhibited better wetting and adhesion on the electrical steel than silicates with less alkali content. The alkali content was limited for structural reasons: too much alkali causes the silicate to crystallize.

2. Firing temperatures between 600°C and 800°C resulted in the best coating microstructure with regard to surface coverage, thickness, and homogeneity, and adhesive flexural strain. Long firing times at elevated temperatures led to loss of adhesive material as the adhesive evaporated, but even after long holding times, some adhesive remained. This suggested that these adhesives would hold up to operating at these elevated temperatures without loss of efficiency.

3. Local inhomogeneities in the adhesive solutions, in the drying process, and in the steel surfaces resulted in a macroscopically uniform but microscopically non-uniform adhesive coating. The resulting coated substrates had areas with higher concentrations of adhesive

41

than others, but the overall structure was an interconnected network of adhesive that would serve to separate the steel sheets. Although homogeneity across the coating was not achievable, satisfactory uniformity as measured by coating thickness was achieved. This allows the steel sheets to be separated by a consistent distance and stacking of these systems to occur. Further, the anisotropy of the steel surfaces did not present a significant limitation in terms of creating a relatively uniform coating.

5.2. Future Work

As an avenue of potential future study, the electrical properties of the coatings should be examined. The sodium silicates are known to be insulating, but the resistance of the system as a whole should be measured to determine any degradation of insulation with loss of the adhesive. It was assumed for the scope of this project that the consistent present of some amount of adhesive would provide the requisite insulation: the steels would always be in contact with either adhesive or air, both of which insulate the layers from one another. A full-scale test of this would be beneficial to realize the limits of this assumption and to understand the extent to which the processing parameters affect the electrical properties of the system as a whole.

Further testing on the mechanical properties of the adhesive under operation conditions should be completed as well before implementation of the coating for the describe applications. These tests may include longer holding times at elevated temperature, flexural strain tests at elevated temperatures, and corrosion tests. The environments under which the adhesives were tested for this project were highly controlled and may not have taken into consideration the conditions the adhesives may be subject to under normal operation. As exposure to harsh environments may degrade the adhesion, the mechanical properties, or the electrical properties of

the adhesives under question, a rigorous analysis of the adhesive's susceptibility to these would

allow the merit of these adhesives to be fully considered.

6. Biographical Notes

Jordan Marks is the daughter of David and E. Joanmarie Marks of Cheyenne, Wyoming. She graduates with a Bachelor of Science in Materials Science and Engineering in June 2014. In her undergraduate studies, she spent two terms at the University of Oxford, taking materials courses and conducting research in a solar group. She served as teaching assistant for two sophomore level classes: the Materials Laboratory course and Microstructural Evolution of Materials. Outside of Materials Science and Engineering, she was heavily involved in public service in the Boston area, particularly through the Museum of Science. She plans to works as a materials and processing engineering for Ball Aerospace & Technologies Corp. following graduation.

7. Acknowledgments

8. References

[1] I. Skeist, Handbook of Adhesives, Springer, 1989.

[2] D. Satas and A. A. Tracton, Coating Technologies Handbook, New York: Marcel Dekker, 2001.

[3] Holo East Ltd., "Adhesive Coating Equipment," HoloEast Ltd., [Online]. Available: http://www.holoeast.com/machines/coating/adhesive-coating-Meyer-Bar.html. [Accessed 15 January 2014].

[4] ASTM International, "Standard Test Methods for Measuring Adhesion by Tape Test," ASTM, 2010.

[5] ASTM International, "Standard Test Methods for Mandrel Bend Test of Attached Organic Coatings," ASTM, 2013.

[6] Paul N. Gardner Co. Inc, "Cylindrical Mandrel Bend Test," GARDCO, [Online]. Available: http://www.gardco.com/pages/impact_flex/mn/pdf/cylindrical_conicalmandrel.pdf. [Accessed 2 February 2014].

[7] ASTM International, "Standard Test Method for Flexural Strength of Advanced Ceramics at Ambient Temperature," ASTM, 2013.

[8] J.T. Baker, "Sodium Silicate Solution Material Safety Data Sheet," J.T.Baker, Center Valley, PA, 2011.

[9] Y. Yuan and T. R. Lee, "Contact Angle and Wetting Properties," in *Surface Science Techniques*, Houston, TX, University of Houston, 2013, pp. 1-34.

[10] T. Young, "An Essay on the Cohesion of Fluids," *Philosophical Transactions of the Royal Society of London,* vol. 98, pp. 65-87, 1805.

[11] A. Marmur, "Wetting on Hydrophobic Rough Surfaces: To Be Heterogeneous or Not To Be?," *Surface Chemistry and Colloids,* vol. 19, no. 20, pp. 8343-8348, 2003.

[12] M. Cima, "Surfaces and Chemical Potential," in *Microstructural Evolution in Materials,* Cambridge, 2011, pp. 15-1 - 15-8.

9. Appendix A

9.1. Development of a Driving Profile

After the adhesive had been applied, it had to be dried to minimize the possibility of water evaporating too quickly off the surface at elevated temperatures and to ensure a uniform coating before increasing the temperature. It was determined that a step-wise profile was most effective at accomplishing this goal, as this allowed water to be evaporated off the surface at low enough rates that the surface did not have bubbles while still allowing a high enough temperature to be reached that the surface completely solidified. The quality of the drying was determined via visual and touch inspection.

9.2. Surface Roughness Measurements

The surface roughness was determined by surface profiling via the HIROX. By taking images from the lowest to the highest focal plane of the steel surfaces, a three-dimensional model of the surface could be constructed, from which the height deviations could be measured. Surface roughness measurements were taken along several lines of the surface, both parallel and perpendicular to the rolling direction. The mean surface roughness measurements were used to computer the total surface area covered by the drops.
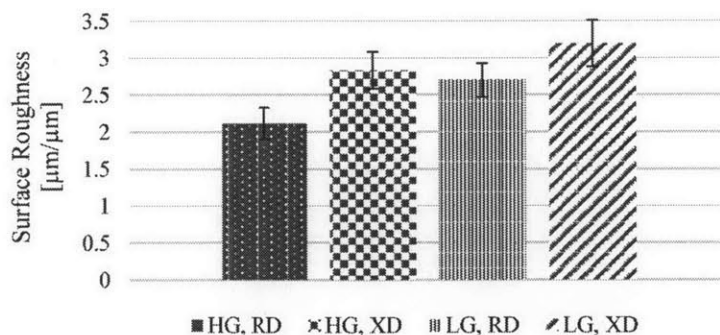

Figure 33. Surface roughness measurements for the steels. HG, LG refer to high and low grade electrical steel respectively. RD, XD refer to the direction parallel and perpendicular to the rolling direction. The cross direction exhibited higher surface roughness. The low grade steel had a higher surface roughness than the high grade steel.

47

It can be seen in Figure 33 that significant variance was involved in the surface roughness measurements. These are due to the measurement method, as well as the presence of surface features as outlined in 274.1.4. For both the low and high grade electrical steels, the surface roughness is higher in the direction perpendicular to the rolling than parallel to rolling (p-values of 0.0006 and 0.01 respectively), as expected based on the observed anisotropy. Furthermore, it can be seen that the low grade electrical steel surfaces are rougher than the high grade electrical steel surfaces (p-values of less than 10^{-6} for both the roll and cross directions) as determined by a pairwise t-test. This also supports the microstructures that were observed due to the differing content of silicon.

The method of surface roughness measurements was limited when determining the roughness. The lowest focal plane was set manually, after which the microscope moved automatically. Because the surface depressions were quite small, determining the lowest focal plane involved some ambiguity. It is assumed that the error follows a standard normal distribution as a result of the focal plane ambiguity.